

## THE FIRST IN-SITU REGOLITH OBSERVATIONS ON THE DELTA FRONT OF JEZERO CRATER, MARS CHARACTERIZED BY THE MARS 2020 SHERLOC AND MASTCAM-Z INVESTIGATIONS

E.L. Cardarelli<sup>1</sup>, A. Vaughan<sup>2</sup>, S. Siljeström<sup>3</sup>, M.E. Minitti<sup>4</sup>, G. Paar<sup>5</sup>, R. Sullivan<sup>6</sup>, D.K. Buckner<sup>7</sup>, E.M. Hausrath<sup>8</sup>, J.R. Johnson<sup>9</sup>, M. Wu<sup>10</sup>, K. Uckert<sup>1</sup>, R. Bhartia<sup>11</sup>, K. Hand<sup>1</sup>, J.F. Bell III<sup>12</sup>, P. Conrad<sup>13</sup>, L. Panossian<sup>1</sup>, and R. Burgos<sup>1</sup>. <sup>1</sup>Jet Propulsion Laboratory, California Institute of Technology, CA. (emily.cardarelli@jpl.nasa.gov), <sup>2</sup>Apogee Engineering, Flagstaff, AZ, <sup>3</sup>RISE Research Institutes of Sweden, Stockholm, Sweden, <sup>4</sup>Framework, Silver Spring, MD, <sup>5</sup>Joanneum Research, Graz, Austria, <sup>6</sup>CCAPS, Cornell University, Ithaca, NY, <sup>7</sup>University of Florida, Gainesville, FL, <sup>8</sup>UNLV, Las Vegas, NV, <sup>9</sup>Johns Hopkins University Applied Physics Laboratory, Laurel, MD, <sup>10</sup>Malin Space Systems, San Diego, CA, <sup>11</sup>Photon Systems Incorporated, Covina, CA, <sup>12</sup>Arizona State University, Tempe, AZ, <sup>13</sup>Carnegie Institution for Science, Washington, DC.

**Introduction:** The Mars 2020 arm-mounted Scanning Habitable Environments with Raman and Luminescence for Organics and Chemicals (SHERLOC) instrument is a deep UV Raman spectrometer that utilizes a 248.6nm pulsed laser. Part of SHERLOC is a color camera known as the Wide Angle Topographic Sensor for Operations and eNginering (WATSON). Together, the SHERLOC suite [1] provides coordinated, spectroscopic and imaging capabilities at high spatial resolution, to detect minerals and organic molecules in a microtextural context. By pairing high spatial resolution (~100 μm) resonance Raman and native fluorescence spectroscopy with microscopic imaging in a novel spacecraft capability, SHERLOC enables texture-specific molecular composition measurements for in-situ regolith (i.e. unconsolidated sediments of variable grain sizes) on Mars. Here we present regolith observations generated with the SHERLOC instrument suite that investigate the diversity of minerals and organic compounds contained within multiple megaripple workspaces, including within the Observation Mountain Workspace where the first Martian regolith core samples were acquired in duplicate for eventual return to Earth via the Mars Sample Return Mission [2].

Linking SHERLOC observations with the stereoscopic, zoomable, and multispectral Mast Camera Zoom (Mastcam-Z) [3,4] observations provides greater geologic context for the spectral detections acquired and facilitates the calculation of key regolith parameters such as the angle of repose and duricrust properties (i.e. height, spatial extent) relevant to the compositional detections from SHERLOC. This work describes the first in-situ regolith observations made within the Delta Front Campaign of the Mars 2020 Mission in Jezero crater by the SHERLOC and Mastcam-Z instrument investigations [1, 3, 4].

**Methods:** For this work, the grain size, distribution, and texture of regolith features were characterized from images generated by the WATSON imaging subsystem of SHERLOC [1] for the targets listed (Table 1). Utilizing the deep-ultraviolet

fluorescence and Raman subsystems of SHERLOC, fluorescence signals consistent with potential organics, along with spectral detections (~100μm resolution) of mineral compositions were mapped onto the target images acquired by the autofocus context imager (10μm/pixel resolution) for select targets (*Topographers\_Peak*, *Marmot\_Bay*, *Ursus\_Cove*).

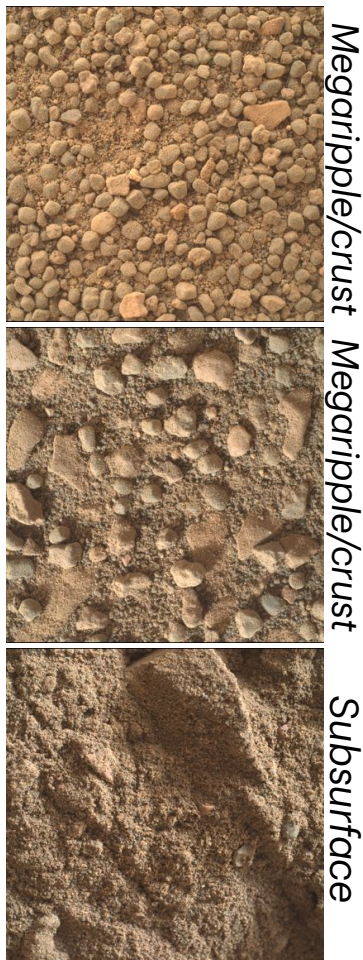
**Table 1.** Delta Front Campaign regolith targets examined in this work, with the sol indicated when SHERLOC spectroscopy was acquired (\*) or coring occurred (\*\*).

Workspace	Sol	Target Name	Details
Amalik	588, 589*	Ursus_Cove	Surface
Observation Mountain	594	Fultons Falls	Surface
	594, 598	Granite_Peak	Surface
	594, 598*	Topographers_Peak	Sub-surface
	594, 598, 600*	Marmot_Bay	Surface
	594, 598, 633, 634**	Atmo_Mountain	Surface
	594, 598, 638, 639**	Crosswind_Lake	Surface
	633	Goodness Bay	Surface

3D models were produced from Mastcam-Z stereo imaging of the workspaces where regolith observations were acquired, thereby generating broader geologic context for the regolith targets examined here.

**Grain characteristics and texture:** Utilizing close-approach WATSON images, size frequency distributions were generated for targets within the Observation Mountain workspace (*Fultons\_Falls*,

**Figure 1.** Regolith targets examined through SHERLOC spectroscopy and WATSON imaging, listed top to bottom (Sol 589 - *Ursus\_Cove*, Sol 600 - *Marmot\_Bay*, Sol 598 - *Topographers\_Peak*).



*Granite\_Peak*, *Atmo\_Mountain*, *Crosswind\_Lake*, *Marmot\_Bay*, *Topographers\_Peak*, *Goodness\_Bay*).

These targets were compared to each other as well as through time, and to the surface of a smaller megaripple (*Ursus\_Cove*) to examine variation between bedforms. Grain-size frequencies were similar among the undisturbed surface targets examined. Within the Observation Mountain workspace, disturbed subsurface regolith (*Topographers\_Peak*) was also compared to the soil crust of the sampled megaripple (*Granite\_Peak*, *Atmo\_Mountain*, *Crosswind\_Lake*, *Marmot\_Bay*, *Goodness\_Bay*, *Fultons\_Falls*). Grain-size frequencies and spectral detections differ between disturbed subsurface regolith, and undisturbed megaripple surficial crust targets.

These results also support grain size distribution gradients within bedforms, as other Mars 2020 studies have reported [5,6]. Chemical composition based

transitions seem to occur with depth belowground. 3D modeling of the Observation Mountain Workspace indicates the presence of a crust (~3.3-3.5 mm in height, Sol 596). There is potential subsurface zonation in the wheel scuff, with a 51.7°-54.7° angle of repose (<https://www.youtube.com/watch?v=tqaDCTZtrcs>).

**Mineralogy, fluorescence, and implications for provenance:** In the surficial targets (Table 1), there are spectral and fluorescence similarities to natural rock surface targets analyzed. Also, the presence of dark rounded grey grains with an olivine-bearing spectral signature are found armoring bedforms in both the Delta Front (Figure 1) Campaign observations as well as in the Crater Floor [5,6] Campaign observations. Prior work indicates that these grains may originate from the olivine-cumulate Séítah unit [6]. Larger 2-5 mm irregularly shaped light toned fragments covering bedforms at the Delta Front are a localized occurrence and appear to be derived from local bedrock.

*Ursus Cove.* 340 nm and 285 nm fluorescence signals are observed in association with fine-grained material, and these detections may be consistent with 1-2 ring aromatics molecules but also possibly with  $Ce^{+}$ .

*Marmot Bay.* Raman detections are consistent with low-forsterite olivine (~800  $cm^{-1}$ ), amorphous silicate (~970  $cm^{-1}$ ), and weathered plagioclase. Fluorescence detections at 335 nm and 285 nm, are apparent predominantly at the grain boundaries. Detections at 335 nm are also apparent on an angular mm sized light-colored grain as well as at grain boundaries.

*Topographers Peak.* Raman spectral signatures are consistent with phosphate, carbonate, sulfates, and weak olivine are also detected. Fluorescence features at 270 nm co-occurring with 285 nm and 335/340 nm fluorescence observed. Fluorescence at 270 nm was also detected in a couple of locations, which has previously only been detected in natural surface bedrock targets.

**Implications for Mars 2020 and beyond:** Overall, this work provides key contextual information for the duplicate regolith samples (*Atmo\_Mountain*, *Crosswind\_Lake*) acquired from the surface of a megaripple for subsequent return to Earth in the upcoming decade.

**Acknowledgments:** We thank the Mars 2020 engineering, operations, and science teams for collectively making the Delta Front observations herein possible.

**References:** [1] Bharita, R., et al. (2020) SSR, 216. [2] Hausrath, E.M., et al. (2022) LPSC 54. [3] Bell, J.F. III., et al. (2020) SSR, 216. [4] Hayes et al. (2021) SSR, 217. [5] Cardarelli, E.L., et al. (2021) LPSC 53. [6] Vaughan et al. (2022) AGU.